Numerical simulation and analysis of mechanized suppression process of seedbed with whole plastic film mulching on double ridges

Fei Dai[1,2], Xuefeng Song[1], Wuyun Zhao[1], Bugong Sun[1*], Ruijie Shi[1], Yang Zhang[1]

(1. *College of Mechanical and Electrical Engineering*, *Gansu Agricultural University*, *Lanzhou 730070*, *China*;
2. *Gansu Provincial Key Laboratory of Aridland Crop Science*, *Gansu Agricultural University*, *Lanzhou 730070*, *China*)

Abstract: In order to achieve the construction standard of high mechanized performance of the seedbed with whole plastic-film mulching on double ridges, in this study, the forms of suppression failure were analyzed, and the key factors influencing the suppression performance were determined based on the structure of the seedbed suppression device and its working principles. The discrete element method was adopted for numerical simulation on the suppression process of the seedbed with whole plastic film mulching on double ridges; the parameters during the interaction between the suppression device and seedbed soil were extracted and analyzed, such as contact area, sinkage and horizontal traction resistance trend of press wheels on big ridges and furrows of small ridge. Taking the suppression load on big ridges, suppression load on furrows of small ridge, and advancing velocity of the combined operation machine as the independent variables, qualified rate of suppression as the response value, a mathematical model between the test factors and qualified rate of suppression was established, to explore the influence sequence of the factors on suppression qualified rate. The optimal working parameters of the suppression device were finally obtained: the suppression load on big ridges was 40 N, suppression load on furrows of small ridge was 69.8 N and the machine advancing velocity was 0.98 m/s, and the achieved mean value of suppression qualified rate was 92.6%. Field verification test showed that the mean value of suppression qualified rate was 90.3%, a mere difference of 2.3% compared with the simulation result. The actual operation of the sample machine was basically consistent with the simulation process and could reveal the mechanized suppression operation mechanism of the seedbed with whole plastic film mulching on double ridges, indicating that the established DEM model and its parameter setting were relatively accurate and reasonable.

Keywords: seedbed, whole plastic film mulching, double ridges, mechanized suppression, discrete element method, numerical simulation, parameter optimization

DOI: 10.25165/j.ijabe.20211401.5866

Citation: Dai F, Song X F, Zhao W Y, Sun B G, Shi R J, Zhang Y. Numerical simulation and analysis of mechanized suppression process of seedbed with whole plastic film mulching on double ridges. Int J Agric & Biol Eng, 2021; 14(1): 142–150.

1 Introduction

Furrows sowing technology with whole plastic film mulching on double ridges is a breakthrough technology in dryland farming in northwest China. The double ridge seedbed covered with whole plastic film integrates the functions of evaporation suppression, rainfall collection and furrows planting, and ensures drought control and production increase to the greatest extent, thus it has been popularized and applied on large scale[1,2]. Therefore, realizing mechanized tillage of double ridge seedbed covered with the whole plastic film is an inevitable trend[3]. Due to its relatively complicated agronomic requirements, especially after mechanized film-mulching and soil covering operation, the whole film laying extends its boundary from the big ridge to furrows and then to the small ridges[4,5]. Therefore, the mechanized suppression operation is of crucial importance: when suppression is too light, the seedbed's ability in resisting wind power from film uncovering would be weakened, resulting in film settlement and insufficient contact; if the suppression is too heavy, then the mulched film may easily slip, resulting in dislocation of film at the center of the big ridges or failure of film-mulching on furrows. Furthermore, the quality of film seeding is reduced and the residual film recovery is restricted. On this account, it is necessary to carry out numerical simulation and analysis on the mechanized suppression process of the seedbed with whole plastic film mulching on double ridges, optimize working parameters of the suppression device and improve its working performance.

The traditional test methods (field test and soil bin test) are mostly adopted in studies on key components of agricultural machinery. At present, software like LS-DYNA, SPH and ABAQUS have been adopted in the operation performance simulation of different types of press wheels[6-8]. The test results of the studies show that exploring the micro-movement of soil at different positions of the seedbed and further comprehend soil disturbance in suppression based on numerical simulation can provide a basis for decision making in the design and optimization of the suppression device. In recent years, with the improvement of soil constitutive model and discrete element algorithm, the simulation test method based on EDEM has been attached greater

Received date: 2020-04-23 **Accepted date:** 2020-11-21

Biographies: Fei Dai, PhD, Associate Professor, research interest: design of agricultural mechanization equipment, Email: daifei@gsau.edu.cn; **Xuefeng Song**, Teaching Assistant, research interest: agricultural mechanization engineering, Email: 549349477@qq.com; **Wuyun Zhao**, PhD, Professor, research interest: agricultural mechanization engineering, Email: zhaowy@gsau.edu.cn; **Ruijie Shi,** PhD candidate, research interest: agricultural mechanization engineering, Email: 1139230110@qq.com; **Yang Zhang**, Lecturer, research interest: agricultural mechanization engineering, Email: zy3537@qq.com.

***Corresponding author: Bugong Sun**, PhD, Professor, research interest: farm machine and mechanical reliability. College of Mechanical and Electrical Engineering, Gansu Agricultural University, Lanzhou 730070, China. Tel: +86-451-7631207, Email: sunbg@gsau.edu.cn.

importance in studying the interaction between soil and contact components, and simulation analysis of all kinds of operation process, such as subsoiling, soil covering, digging, rotary tillage has been done[9-11], however, there are few studies on the numerical simulation of the mechanized suppression process of the seedbed with whole plastic film mulching on double ridges, therefore, it is necessary to reveal the operation mechanism based on the research method.

For this reason, by establishing a 3D model on the interaction between the rigid suppression device (big ridge press wheels and press wheel on small ridge furrows) and seedbed soil, a discrete element method was applied to study the dynamic suppression process. Taking a load of the press wheel for the big ridge and load of the press wheels for small ridge furrows and the advancing velocity as test factors, suppression qualified rate of seedbed as test index, the study was aimed at revealing the mechanism of mechanized suppression of the seedbed with whole plastic film mulching on double ridges, to provide a theoretical basis for establishing a seedbed with whole plastic film mulching on double ridges.

2 Suppression device and its working principle

2.1 Structure

The suppression device on the double-ridge seedbed is the key component of the combined machine for whole plastic film mulching on double ridges (Figure 1). It is mainly composed of a body frame, press wheel for the big ridge and press wheel for the small ridge furrows. In order to meet the agronomic requirements in establishing a mechanized seedbed of whole plastic-film mulching on double ridges, the double-ridge seedbed suppression device has two groups of big ridge press wheels and press wheels of small ridge furrow, which are in symmetrical arrangement[12].

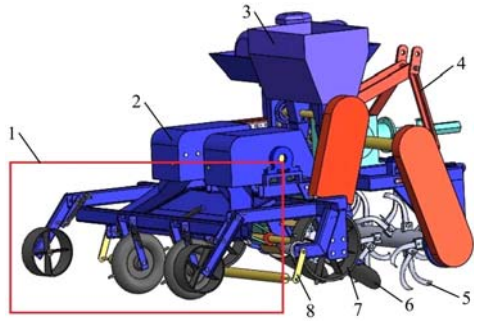

a. Structure of the machine

b. The suppression device on the double-ridge seedbed

1. Double-ridge seedbed suppression device 2. Soil covering device 3. Fertilizer 4. Hanger 5. Rotary tillage device 6. Ridge forming device 7. Walking device 8. Film-mulching device

Figure 1 Structure of the whole plastic film ridging and mulching machine on double ridges

The double-ridge seedbed suppression device as one of the key components in the ridge forming and film-mulching machinery is equipped in machinery such as simple type and combined ridge forming and film-mulching machine. With the coordination of the press wheel and perforating wheel, the operations such as ridge pressing, soil covering, and perforating for water infiltration, its working performance not only directly affects the shape of ridges and mulching film after pressing, but also affects the soil compactness as well as the contact tightness between fertilizer particles and soil, thus impact the ridge forming and film-mulching quality and seeding quality and crop growth and its yield.

2.2 Mechanized ridge suppression process and agronomic requirements

The agronomic requirements in the mechanized ridge suppression process are shown in Figure 2. During mechanized film-mulching, taking the small ridge as the central baseline, a white mulching film of 1200 mm in width was laid, that is, the whole film covers the small ridge and the furrows on both sides, as well as half of the big ridges on both sides, meanwhile, with the coordination of the lateral channel, direct channel and suppression device, soil covering and suppression is finished on film edges and furrows[4].

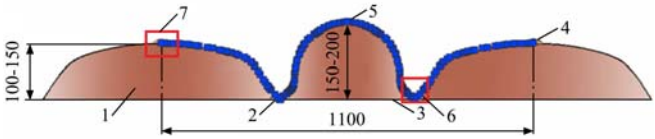

1. Big ridge 2. Soil covering belt 3. Small ridge 4. Central soil belt on big ridge 5. Whole plastic film covering 6. Suppression position on small ridge furrow 7. Suppression position on big ridge

Figure 2 Agronomic requirements of mechanized film-mulching of the whole plastic film mulching on double ridges

Among them, the suppression position on big ridges and the small ridge furrows are shown in the red box in Figure 3. In the suppression process along with film-mulching and soil covering, if the load of the press wheels on the big ridges is too high, the soil belt on the big ridge center would sink (Figure 3a) and at this time the whole film on the ridge would slip sideward, and the film at the soil belt in the furrows would be lifted, causing off-contact between soil and film in the small ridge furrow; if the load of the press wheels on the small ridge furrows is too high, the soil belt in both furrows would sink (Figure 3b), and at this time, the whole film shrinks to both sides of the small ridge, and the film at the soil belt at the center of the big ridges is pulled away, causing failure of docking of film edges in soil covering. Also, if the soil belts on the big ridges are too wide, thus the evaporation suppression and rainfall collecting functions would be undermined.

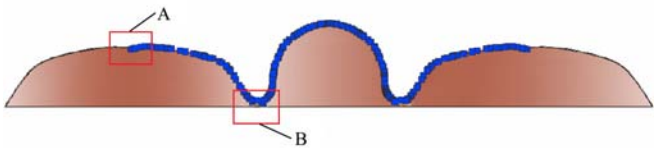

a. Suppression failure I

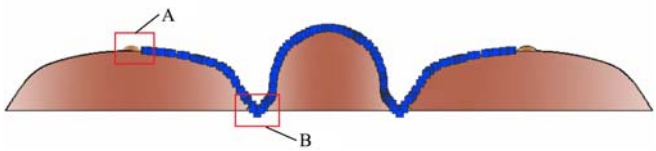

b. Suppression failure II

Figure 3 Failure mode of seedbed mechanized suppression

2.3 Suppression device resistance analysis in suppression process

When the seedbed suppression device is rolling forward on the double-ridge soil covered with the whole film, there are power consumptions in suppression resistance, pushing resistance and

adhesion resistance. Among them, the power consumed by suppression resistance R_c is equal to that consumed in forming ditched on seedbed soil or punching seepage holes, suppression resistance R_c is directly related to sinkage of suppression roller. The calculation equation of suppression resistance R_c can be obtained by reference [6]:

$$\begin{cases} R_c = KB\dfrac{z^{n+1}}{n+1} \\ K = \dfrac{k_c}{B} + k_\tau \\ z = \left[\dfrac{3W}{(3-n)KB\sqrt{D}}\right]^{\frac{2}{2n+1}} \end{cases} \quad (1)$$

where, K is non-elastic deformation modulus; k_c is the characteristics parameter related to the cohesive force of soil; k_τ is the characteristics parameter related to soil friction; B is the width of press wheel, mm; n is sinkage index; z is sinkage of the press wheel, mm; W is the load of the press wheel (including the dead weight of the press wheel), kg; D is the diameter of the press wheel, mm.

It can be obtained by analyzing Equation (1) that, other than the physical and mechanical characteristics of seedbed soil, the factors that affect the suppression resistance of the seedbed suppression device are the structural dimensions of the device, sinkage and suppression load. Therefore, in a follow-up study, it is reasonable to take press wheel load on the big ridges, press wheel load on the small ridge furrows and the machine advancing velocity as test factors and suppression qualified rate as test index to study the mechanized suppression mechanism of seedbed with whole plastic film mulching on double ridges.

3 Mechanized suppression simulation test on the seedbed with whole plastic film mulching on double ridges

3.1 Establishment of the model of mechanized seedbed suppression device

In order to further analyze the dynamic interaction characteristics between different types of press wheels and soil in the mechanized suppression process of the seedbed, in this study, discrete element method was adopted for numerical simulation of the suppression process. A soil bin cubic of 2000 mm×1800 mm×600 mm was established in the EDEM software and named wall. Choose the material of the wall as steel, and set the 3D model material of the double-ridge seedbed as virtual, then the cubic completely wraps up the double-ridge seedbed model. According to the preliminary research foundation of our group, the static particle generation method was adopted in the wall to generate soil particles with a diameter of 3 mm, the filing height of particles reached the upper edge of the wall in +z direction[13]. According to the structural requirement of seedbed with whole plastic film mulching on double ridges, the press wheel set includes a pair of big ridge press wheels (steel) and a pair of press wheels on small ridge furrows (rubber), in which the diameter of the big ridge press wheels is 200 mm, wheel width is 80 mm, the diameter of press wheel on small ridge furrows is 180 mm with wheel width of 60 mm, and there are punching teeth at the wheel flange of 35 mm in height, diameter of the circular section of the teeth root is 10 mm. The established discrete element model for mechanized suppression of the seedbed with whole plastic film mulching on double ridges is shown in Figure 4.

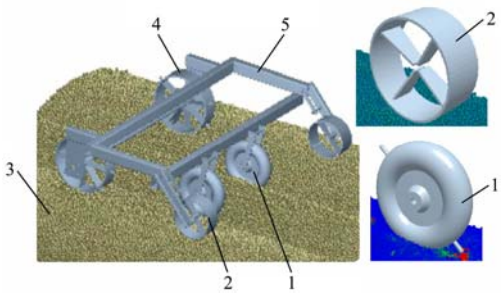

1. Press wheels on small ridge furrows 2. Big ridge press wheels 3. Seedbed with whole plastic film mulching on double ridges 4. Walking ground wheels 5. Body frame

Figure 4 Discrete element model of the seedbed with whole plastic film mulching on double ridges

In the discrete element model of the seedbed with whole plastic film mulching on double ridges, Hertz-Mindlin (no-slip) was chosen as the contact model of soil particle-soil particle, soil particle-big ridge press wheel (steel), soil particle-small ridge press wheel (rubber). According to the preliminary research basis and simulation test, the parameter setting is shown in Table 1[5,14-19].

Table 1 Parameters of materials and contact

Items	Parameters	Numerical values
Soil particles	Poisson's ratio	0.40
	Shear modulus/Pa	1.0×10^6
	Density/kg·m^{-3}	1364
Big ridge press wheels	Poisson's ratio	0.28
	Shear modulus/Pa	3.5×10^{10}
	Density/kg·m^{-3}	7850
Press wheels on small ridge furrows	Poisson's ratio	0.49
	Shear modulus/Pa	2.6×10^5
	Density/kg·m^{-3}	1300
Soil particle-soil particle	Recovery coefficient	0.20
	Static friction coefficient	0.4
	Dynamic friction coefficient	0.30
Soil particles-big ridge press wheel	Recovery coefficient	0.30
	Static friction coefficient	0.4
	Dynamic friction coefficient	0.10
Soil particle-press wheels on small ridge furrows	Recovery coefficient	0.25
	Static friction coefficient	0.4
	Dynamic friction coefficient	0.05

3.2 Numerical simulation of mechanized ridge suppression

Solidworks was used to create the geometric simulation model of the ridge forming device, which was then imported into the EDEM software. The numerical simulation process of mechanized ridge forming is shown in Figure 5, the simulation time step is 1.23×10^{-5} s, and the total simulation time is 2.50 s[20,21].

As shown in Figures 5a-5f, when the advancing velocity of the combined machine was 0.75 m/s, the press wheel load on the big ridges was 50 N, the press wheel load of the small ridge furrow was 80 N, and the time t=0.10-2.50 s, the mechanized suppression process of whole plastic film mulching on double ridges was numerically simulated. The observation of the interaction between the suppression device and seedbed soil should be started after stable contact is achieved between the device and soil, therefore, from t = 0.10 s, the EDEM numerical simulation approaches the working status of mechanized suppression, as shown in Figure 5a. When t=0.50 s, the suppression device started to go forward on the whole plastic film mulched seedbed on

double ridges. Due to the gravity of the device, wheel mark was produced at the soil belt on big ridge center by the press wheel, and soil sinkage was obvious (Figure 5b). When t = 1.00 s, the suppression device went forward on the seedbed with whole plastic film mulching on double ridges, and obvious soil sinkage also occurred in the furrow under the pressure from the ground wheel (Figure 5c), the wheel teeth penetrated into soil and dug out soil particles in circular motion and discretized some of the soil particles in the seedbed. From t =1.50-2.50 s (Figures 5d, 5e, 5f), the mechanized suppression process of the seedbed with whole plastic film mulching on double ridges gradually became stable, and the traction resistance of the suppression device, contact area between the wheels and seedbed as well as sinkage of the seedbed basically came into a stable state.

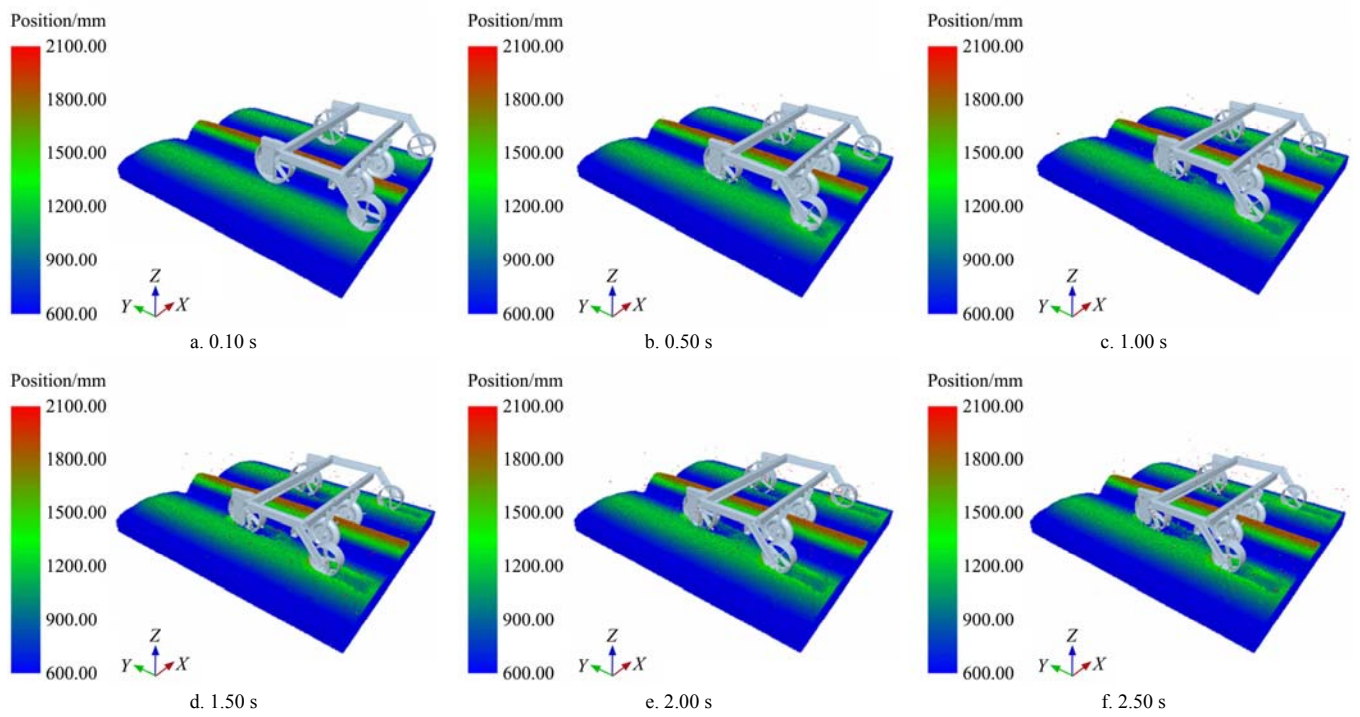

a. 0.10 s b. 0.50 s c. 1.00 s

d. 1.50 s e. 2.00 s f. 2.50 s

Figure 5 Numerical simulation of the mechanized suppression process of seedbed with whole plastic film mulching on double ridges

3.3 Contact area of press wheels

Figure 6 shows the variation curves of contact areas between press wheels on big ridges, press wheels on small ridge furrows and the seedbed with whole plastic film mulching on double ridges respectively[6,7].

It can be observed from the variation curve of contact area of big ridge press wheels (Figure 6a) that, before t=0.40 s, the contact area between the big ridge press wheel and the seedbed was on the increase with the increased machine-soil interaction degree. With the continuous advancements of the suppression device on the seedbed (t=0.50-1.25 s), the contact area of the big ridge press wheel was kept between 0.022-0.026 m^2 in a corrugated changing trend. After t=1.50 s in simulation, the contact area of the big ridge press wheels kept a stable trend between 0.020-0.023 m^2, showing a stable suppression process on big ridge in this stage. The variation trend of contact area of the press wheel on small ridge furrows was basically consistent with that of the big ridge press wheels (Figure 6b), however, constrained by the structural dimensions of the press wheel on small ridge furrows, its contact area with seedbed soil was smaller than that of the big ridge press wheels on the whole. Meanwhile, with the four-point support by the walking ground wheels and big ridge press wheels, the press wheels on small ridge furrows walked in a stable state; after t=0.80 s in simulation, the contact area between the press wheel of small ridge furrow and the seedbed kept between 0.012-0.013 m^2.

3.4 Press wheel sinkage

Figure 7 shows the variation curves of contact areas between press wheels on big ridges, press wheels on the small ridge furrow and the seedbed with whole plastic film mulching on double ridges respectively. Among them, in the variation of sinkage of the big ridge press wheels, with the instantaneous contact between the suppression device and the seedbed soil, the sinkage rapidly increased and reached the maximum value at t=0.30 s. When the big ridge press wheels continued to go forward, the soil under the wheels was extruded and deformed, the soil behind the soil had plastic deformation. The farther the soil from the soil surface, the weaker the deformation was. Therefore, the variation of sinkage of the big ridge press wheels presented a trend of a drop after an increase; after t=1.25 s, the sinkage of the big ridge press wheels became stable and kept at around 9.8 mm.

Compared with the big ridge press wheels, the variation trend of sinkage of the press wheel on small ridge furrows was relatively gentle. With the instantaneous contact between the suppression device and seedbed soil, the sinkage increased sharply and reached the maximum value (5.4 mm). When t = 0.50 s, and then the variation tendency of sinkage became basically stable. The variation curve of sinkage of the press wheel on small ridge furrows shows that it kept a fluctuation state of micrometric displacement with the passage of time, which is associated with the intermittent penetration of the punch tines on the wheels into the film-soil complex.

The sinkage variation curves of the suppression device above show that the established model of the mechanized suppression device was accurate and reasonable and can be applied in parameter optimization of the device in future research.

3.5 Horizontal traction resistance

The resistance on the suppression device mainly comes from the suppression of the big ridges and small ridge furrows[7,22]. Figure 8 shows the variation curves of the horizontal traction

resistance on the suppression device, and the component force of the resistance on the device in the forward direction was traction resistance. The variation curve of the horizontal traction resistance on the big ridge press wheels shows that, when the press wheels were pressing forward on the big ridges, the horizontal traction resistance changed between the range of 30.6-67.8 N, after t=2.00 s, the horizontal traction resistance on the big ridge press wheels became stable and kept at 50 N.

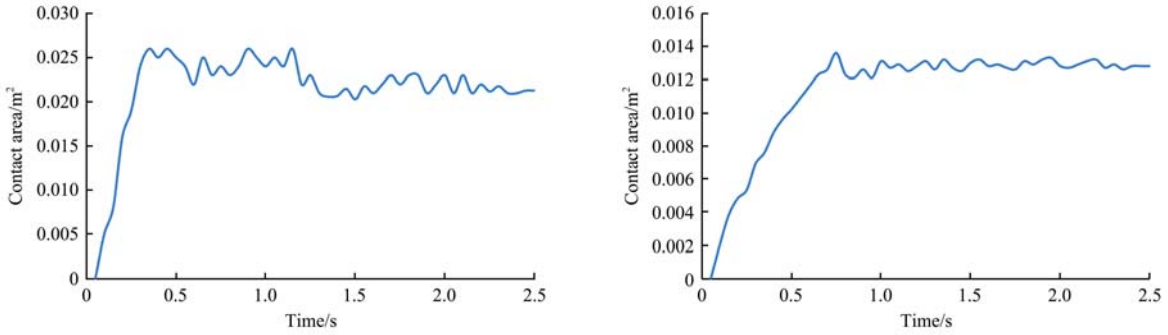

a. Variation curve of contact area of a big ridge press wheel b. Variation curve of contact area of a press wheel of small ridge furrow

Figure 6 Variation curves of contact areas of the suppression device

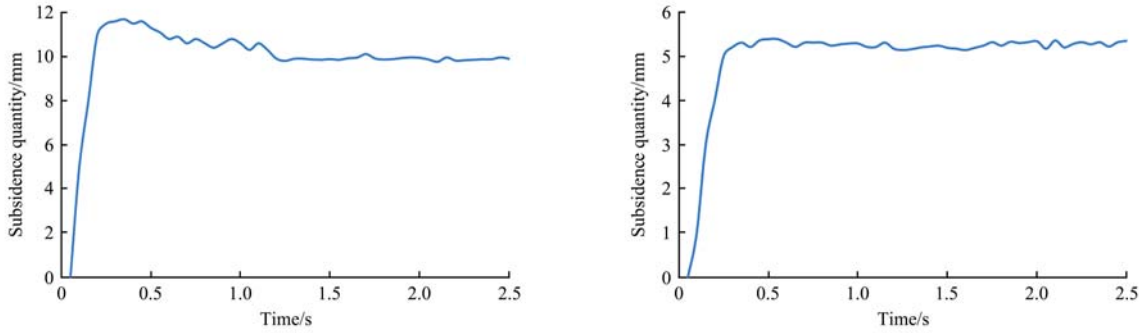

a. Variation curve of sinkage of big ridge press wheels b. Variation curve of sinkage of press wheel on small ridge furrows

Figure 7 Variation curves of sinkage of the suppression device

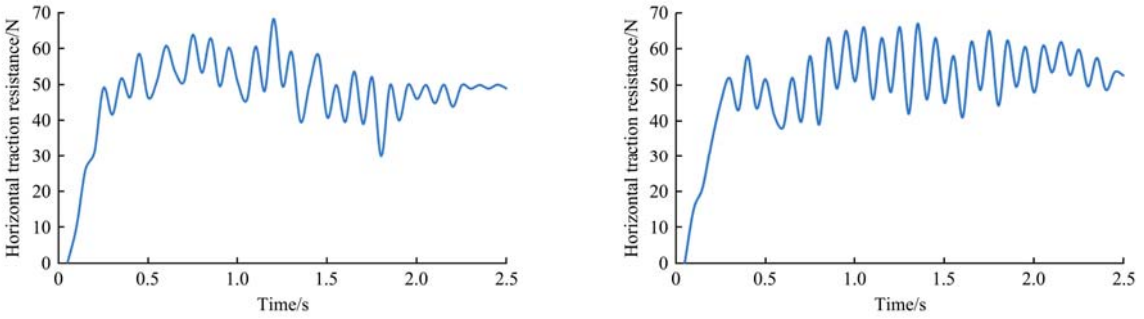

a. Variation curve of horizontal traction resistance on big ridge press wheels b. Variation curve of horizontal traction resistance on press wheel of small ridge furrow

Figure 8 Variation curves of horizontal traction resistance on the suppression device

Affected by the punch tines, the fluctuation of horizontal traction resistance on the press wheels on small ridge furrows kept within the range of 36.1-68.2 N, which was more evident compared with that on big ridge press wheels; after t=2.00 s, the horizontal traction resistance on the press wheels on small ridge furrows became relatively stable and still kept within 48.6-60.8 N.

4 Parameter optimization of the mechanized seedbed suppression device

4.1 Test design and method

The numerical simulation test of the seedbed with whole plastic film mulching on double ridges was carried out by referring to the standard NY/T 987-2006 Operating quality of film-covered hill-drop drill, in which the sinkage≤15 mm after suppression on the big ridges and small ridge furrows was determined as the qualified standard. By taking the qualified rate of seedbed suppression as the evaluation index, the working parameter optimization simulation test on the suppression device was carried out. Based on the simulation model established in Figure 9, the sinkage after suppression at different positions of the seedbed was measured after each simulation test, and the qualified rate of seedbed suppression was calculated. The formula for determining the qualified rate of seedbed suppression is

$$Y = \frac{Z_1}{Z} \times 100\% \quad (2)$$

where, Y is the seedbed suppression qualified rate, %; Z_1 is the test points in seedbed suppression; Z is the total test points.

Based on the variation curves of press wheel contact area, sinkage and horizontal traction resistance, the suppression load on big ridges x_1 (40-60 N), suppression load on small ridge furrow x_2 (60-80 N) and advancing velocity of the combined machine x_3 (0.50-1.00 m/s) were taken as test factors, and qualified rate of

seedbed suppression Y was taken as evaluation index in the test. The three-factor and three-level response surface method was adopted in the test and the level codes of the test factors are shown in Table 2. 17 groups of response surface analysis tests were carried out (Table 3) and each group of tests was repeated three times. The mean values of the three test results were taken as final test results for data processing and analysis by the software Design-Expert 8.0.6.1.

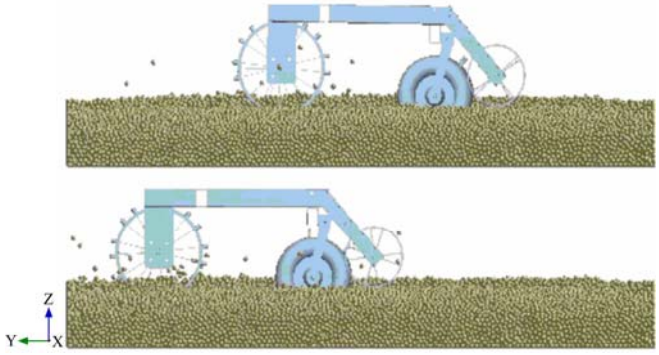

Figure 9 Establishment of the model of mechanized seedbed suppression device

Table 2 Coding of factors and levels

Coding table	Factors		
	Suppression load on the big ridges x_1/N	Suppression load on the small ridge furrows x_2/N	Advancing velocity of the combined machine x_3/m·s^{-1}
−1	40	60	0.50
0	50	70	0.75
1	60	80	1.00

4.2 Establishment and test of regression model

The test results are shown in Table 3. The qualified rate of seedbed suppression was among 88.2%-89.7%, showing that the suppression variation of the established model in the simulation test was stable and the model was reliable.

Table 3 Results of response surface analysis

Test No.	X_1	X_2	X_3	Y/%
1	–1	1	0	89.4
2	1	–1	0	88.2
3	0	0	0	89.3
4	–1	0	1	89.7
5	–1	0	–1	89.1
6	1	0	–1	88.4
7	0	0	0	89.3
8	1	0	1	88.7
9	0	–1	–1	88.6
10	0	1	–1	88.9
11	0	–1	1	89.0
12	–1	–1	0	89.4
13	1	1	0	88.6
14	0	0	0	89.3
15	0	0	0	89.4
16	0	0	0	89.3
17	0	1	1	89.2

Design-Expert 8.0.6.1 was used to analyze test results, and the quadratic regression model of qualified rate Y of seedbed suppression expressed by coding values was obtained:

$$Y = 89.32 - 0.46X_1 + 0.11X_2 + 0.20X_3 - 0.19X_1^2 - 0.24X_2^2 - 0.16X_3^2 + 0.10X_1X_2 - 0.075X_1X_3 - 0.025X_2X_3 \quad (3)$$

where, Y is the seedbed suppression qualified rate, %; X_1 is the coding value of the suppression load on big ridges; X_2 is the coding value of the suppression load on small ridge furrows; X_3 is the coding value of the advancing velocity of the combined machine.

Variance analysis and significance testing on the regression coefficients were made on the quadratic regression model, and the results are shown in Table 4.

Table 4 Variance analysis of regression equation

Source of variation	Sum of squares	Degree of freedom	Mean square	F	P
Regression	2.74	9	0.300	83.48	<0.0001**
X_1	1.71	1	1.710	469.75	<0.0001**
X_2	0.10	1	0.100	27.79	0.0012**
X_3	0.32	1	0.320	87.84	<0.0001**
X_1X_2	0.040	1	0.040	10.98	0.0129*
X_1X_3	0.023	1	0.023	6.18	0.0419*
X_2X_3	2.50×10^{-3}	1	2.500×10^{-3}	0.69	0.4348
X_1^2	0.14	1	0.140	39.56	0.0004**
X_2^2	0.23	1	0.230	63.83	<0.0001**
X_3^2	0.11	1	0.110	29.59	0.0010**
Residual error	0.025	7	3.643×10^{-3}		
Lack-of-fit	0.017	3	5.833×10^{-3}	2.92	0.1639
Error	8.00×10^{-3}	4	2.000×10^{-3}		
Sum	2.76	16			

Note: * significant (p <0.05) and ** extremely significant (p<0.01).

According to the analysis in Table 4, the quadratic regression model p<0.0001, which indicates that the regression model is very significant; Lack of fit p>0.05, i.e., the Lack of fit is not significant, which indicates that the quadratic regression equation fitted by the model is consistent with the actual situation, and can accurately reflect the relationship between the qualified rate of seed-bed suppression Y and factors X_1, X_2 and X_3. The regression model can be used to predict the results of various experiments in the optimization test. The first item X_1 (suppression load on big ridges), the second item X_2 (suppression load on small ridge furrow) and X_3 (advancing velocity of the combined machine) and the quadratic terms X_1^2, X_2^2 and X_3^2 had extremely effects on the suppression rate of the seedbed; the interaction items X_1X_2 and X_1X_3 had significant influence, and the other items were not significant. According to the regression coefficient of each factor of the model, the main order of the influence of each factor on the qualified rate of suppression is X_1, X_3, X_2, that is, suppression load on the big ridges, the advancing velocity of the combined machine and the suppression load on the small ridge furrows.

4.3 Analysis of interaction items of the model

According to the quadratic regression model (3), a response surface diagram of the relationship of all test factors can be drawn, and the shape of the response surface can reflect the influence of interaction factors. From the results in Table 4, among the three test factors, it can be found that the interaction between suppression loads on both big ridges and small ridge furrow, interaction between suppression load on big ridges and advancing velocity of the combined machine had a significant effect on the qualified rate of seedbed suppression, while the influence of other interactive factors (X_2X_3) was not significant, the p (0.4348) value>0.05. Thus a response surface of two pairs of interactive factors was made, as shown in Figure 10 and Figure 11.

As can be seen from Figure 10 that, with the suppression load on small ridge furrow fixed at a certain level, the suppression load

on the big ridges increased from 40 N to 60 N, the qualified rate of seedbed suppression was on the decline. The reason is that, with the increase of suppression load on big ridges, the central soil belts on big ridges would sink, at this time, the whole mulching film on the ridges was pulled sideward, and the film on the small ridge furrows was lifted, causing off-contact between soil and film and unqualified seedbed suppression.

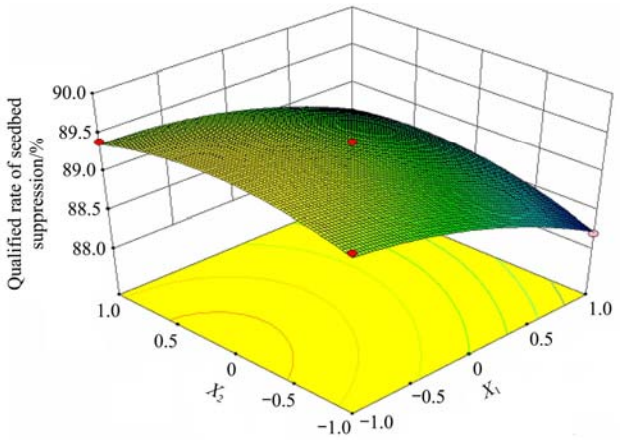

Figure 10 Influence of suppression loads on big ridges and small ridge furrows on qualified rate of seedbed suppression

As can be seen from Figure 11, with the suppression load on big ridges fixed at a level, when the advancing velocity of the combined machine increased from 0.50 m/s to 1.00 m/s, the qualified rate of seedbed suppression was on the increase. The reason is that, with the gradual increase of the advancing velocity of the combined machine in the suppression process, the instantaneous interaction time shortened between big ridge press wheels, press wheel of small ridge furrows and the seedbed, and the soil sinkage of big ridges and small ridge furrow per unit time was reduced, thus the qualified rate of seedbed suppression was elevated.

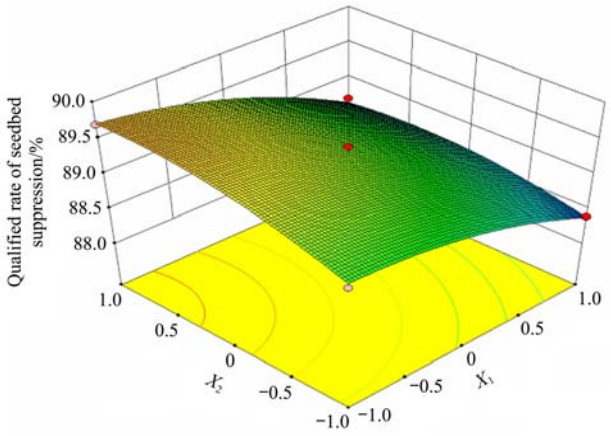

Figure 11 Influence of suppression load on big ridges and advancing velocity of the combined machine on qualified rate of seedbed suppression

Figure 12 shows the seedbed suppression process of the suppression device under different views in the fourth group of tests shown in Table 3, when the suppression load on big ridges was 40 N, the suppression load on small ridge furrow was 70 N and the advancing velocity of the combined machine was 1.00 m/s, and at this time, the qualified rate of seedbed suppression was 89.7%. It was able to show the actual test process more realistically, and the interaction between the two kinds of press wheels and the soil in different ridge could be well demonstrated.

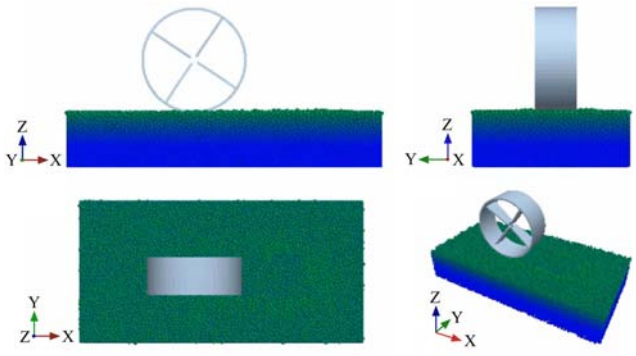

a. Interaction between the big ridge press wheels and seedbed soil

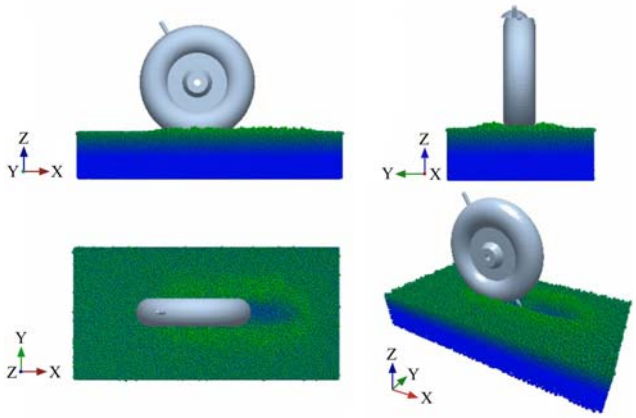

b. Interaction between the press wheel of small ridge furrow and seedbed soil

Figure 12 Interaction between the suppression device and seedbed soil

4.4 Parameter optimization of the mechanized seedbed suppression device

Taking the full qualified rate of seedbed suppression operation as the target, the Optimization-Numerical module was applied for optimization solution on the regression equation Model (3) to achieve the target. The optimal working parameters of the suppression device were as follows: the suppression load on big ridges was 40 N, the suppression load on small ridge furrow was 69.8 N, and the advancing velocity of the combined machine was 0.98 m/s.

In order to verify the reliability of Model (3), the optimal working parameters of the suppression device was adopted for the seedbed suppression performance simulation test (Figure 13). Test results showed that the average suppression qualified rate in the simulation test was 92.6%, an evident increase before the optimization, showing that the coordinated loads by the press wheels on big ridges and small ridge furrow can be applied under optimal working parameters, to avoid horizontal slippage and vertical tearing under mechanized press wheel set and alleviate the disturbance on seedbed mulching, ensure the stability of mechanized seedbed of the whole plastic-film on double ridges, so as to further reduce the dislocation rate of soil hole in seeding. Therefore, the established regression model on the seedbed suppression qualified rate was reliable.

5 Field test verification

In order to further verify the suppression performance of the suppression device under the optimal working parameters, a verification test was carried out in the experimental field of Taohe Tractor Manufacturing Co., Ltd. of Lintao County, Dingxi City, Gansu Province in June 2019 (Figure 14), and working conditions of the test site and test method can be referred to in reference [23],

the soil type was loessal soil, the soil moisture content was 16.86%, the soil bulk density is 1300 kg/m^3 and the soil firmness <0.20 MPa. After the suppression test, a seedbed of 15 m in length of whole plastic-film mulching on double ridges was randomly selected for measurement, and the average values of 6 operation plots were taken as test results. Test results showed that the average suppression qualified rate was 90.3%.

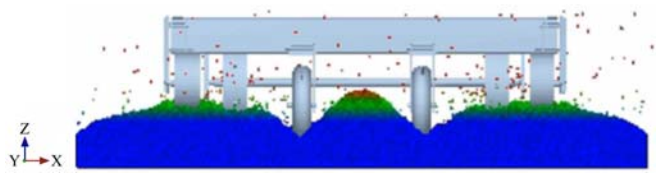

a. Front view

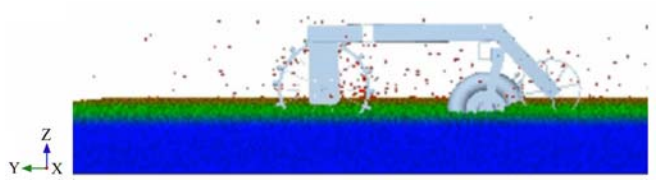

b. Left view

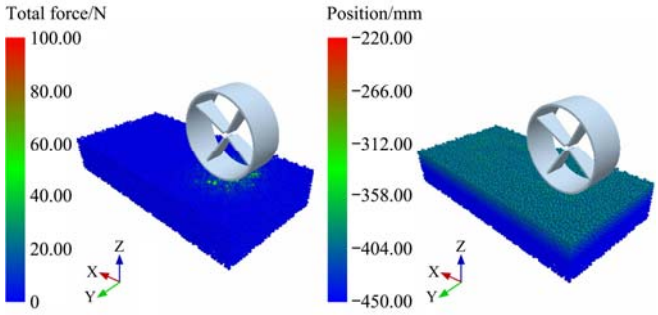

c. Compacting force and sinkage displacement in the interaction between the big ridge press wheels and seedbed soil

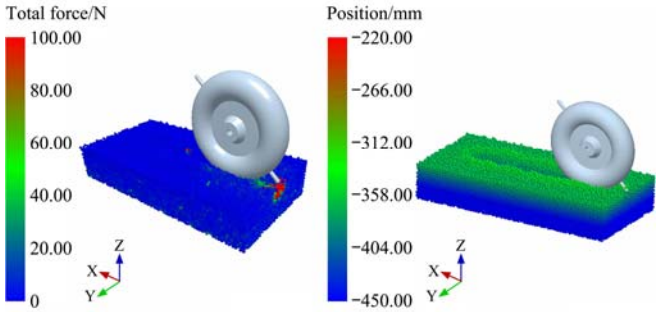

d. Compacting force and sinkage displacement in the interaction between press wheel of small ridge furrows and seedbed soil

Figure 13 Simulation test on seedbed suppression performance under the optimal working parameters of the suppression device

Figure 14 Field performance test of seedbed suppression

It was found in the test that, with the coordination of loads of the big ridge press wheels and press wheel of small ridge furrow, the whole plastic-film mulching on double ridges could cover ridges and furrow in close contact without slippage. Meanwhile, the suppression on the soil belt at the center of the big ridges was smooth without any dislocation or off-contact between soil and the film.

Due to the great difference between parameters of soil particles and agglomeration degree of actual seedbed soil in establishing the seedbed model based on discrete element method, without taking account of the variation of soil moisture content and soil hardness, the actual interaction between the suppression device and seedbed soil cannot be fully presented, and in the simulation process of suppression, there was still slippage and ridge collapse, therefore, it is necessary to further optimize the established model and related parameters.

6 Conclusions

1) In this study, the forms of suppression failure were analyzed, and the key factors influencing the suppression performance were determined based on the structure of the seedbed suppression device and its working principles. Next, discrete element method was adopted for numerical simulation on the suppression process of the seedbed with whole plastic film mulching on double ridges; and the parameters during the interaction between the suppression device and seedbed soil were extracted analyzed, such as contact area, sinkage and horizontal traction resistance trend of press wheels on big ridge and furrows of small ridges.

2) Response surface analysis method was applied to establish a quadratic polynomial regression model on the qualified rate of seedbed suppression, big ridge suppression load, small ridge furrow suppression load and the advancing velocity of the combined machine. Taking the full qualified rate of seedbed suppression operation as the target, the optimal working parameters of the suppression device were as follows: the suppression load on big ridges was 40 N, the suppression load on small ridge furrow was 69.8 N, and the advancing velocity of the combined machine was 0.98 m/s. Under the optimal working parameters, the average qualified rate of seedbed suppression operation was 92.6%.

3) Field verification test showed that the mean value of suppression qualified rate was 90.3%, a mere difference of 2.3% compared with the simulation result. The actual suppression operation of the sample machine was basically consistent with the simulation process and could reveal the mechanized suppression operation mechanism of the seedbed with whole plastic film mulching on double ridges, indicating that the established DEM model and its parameter setting were relatively accurate and reasonable.

Acknowledgements

The authors acknowledge that this work was financially supported by the National Natural Science Foundation of China (Grant No. 51775115; No. 52065005), Outstanding Youth Foundation of Gansu Province (Grant No. 20JR10RA560), Natural Science Foundation of Gansu Province (Grant No. 20JR5RA029), Research Program Sponsored by Gansu Provincial Key Laboratory of Aridland Crop Science, Gansu Agricultural University (Grant No. GSCS-2020-01),.

[References]

[1] Zhou L M, Jin S L, Liu C A, Xiong Y C, Si J T, Li X G, et al. Ridge-furrow and plastic-mulching tillage enhances maize-soil interactions: opportunities and challenges in a semiarid agroecosystem. Field Crops Research, 2012; 126: 181–188.

[2] Gan Y T, Siddique K H, Turner N C, Li X G, Niu J Y, Yang C, et al. Chapter Seven-Ridge-furrow mulching systems-an innovative technique for boosting crop productivity in semiarid rain-fed environments.

Advances in Agronomy, 2013; 118(1): 429–476.
[3] Dai F, Zhao W Y, Zhang F W, Ma H J, Xin S L, Ma M Y. Research progress analysis of furrow sowing with whole plastic-film mulching on double ridges technology and machine in northwest rainfed area. Transactions of the CSAM, 2019; 50(5): 1–16. (in Chinese)
[4] Dai F, Zhao W Y, Zhang F W, Wu Z W, Song X F, Wu Y F. Optimization and experiment of operating performance of collector for corn whole plastic film mulching on double ridges. Transactions of the CSAE, 2016; 32(18): 50–60. (in Chinese)
[5] Dai F, Guo W J, Song X F, Shi R J, Zhao W Y, Zhang F W. Design and test of crosswise belt type whole plastic-film ridging-mulching corn seeder on double ridges. Int J Agric & Biol Eng, 2019; 12(4): 88–96.
[6] Liu H J, Han J Y, Chen J Q, Lyu J Q, Zhao S H. Performance simulation and experiment on rigid press wheel for hilly area. Transactions of the CSAE, 2018; 49(11): 114–122. (in Chinese)
[7] Zhao S H, Liu H J, Tan H W, Yang Y Q, Zhang X M. Design and experiment of bidirectional profiling press device for hilly area. Transactions of the CSAE, 2018; 49(11): 114–122. (in Chinese)
[8] Tong J, Zhang Q Z, Chang Y, Li M, Zhang L L, Liu X. Finite element analysis and experimental verification of bionic press roller in reducing adhesion and resistance. Transactions of the CSAE, 2014; 45(7): 85–92. (in Chinese)
[9] Ucgul M, Fielke J M, Saunders C. 3D DEM tillage simulation: validation of a hysteretic spring (plastic) contact model for a sweep tool operating in a cohesionless soil. Soil and Tillage Research, 2014; 144(4): 220–227.
[10] Ucgul M, Fielke J M, Saunders C. Comparison of the discrete element and finite element methods to model the interaction of soil and tool cutting edge. Biosystems Engineering, 2018; 169: 199–208.
[11] Tamas K. The role of bond and damping in the discrete element model of soil-sweep interaction. Biosystems Engineering, 2018; 169: 57–70.
[12] Dai F, Zhao W Y, Shi R J, Zhang F W, Ma H J, Ma M Y. Design and experiment of operation machine for filming and girdle covering on double ridges. Transactions of the CSAM, 2019; 50(6): 130–139. (in Chinese)
[13] Dai F, Zhao W Y, Song X F, Zhang F W, Feng F X. Working process analyses of direct insert hill-device with corn whole plastic-film mulching on double ridges based on EDEM. International Agricultural Engineering Journal, 2017; 26(4): 124–131.
[14] Ucgul M, Fielke J M, Saunders C. Three-dimensional discrete element modelling of tillage: determination of a suitable contact model and parameters for a cohesionless soil. Biosystems Engineering, 2014; 121(2): 105–117.
[15] Zhao Z, Li Y M, Liang Z W, Gong Z Q. DEM simulation and physical testing of rice seed impact against a grain loss sensor. Biosystems Engineering, 2013; 116: 410–419.
[16] Oldal I, Safranyik F. Extension of silo discharge model based on discrete element method. Journal of Mechanical Science & Technology, 2015; 29(9): 3789–3796.
[17] Qi L, Chen Y, Sadek M. Simulations of soil flow properties using the discrete element method (DEM). Computers and Electronics in Agriculture, 2019; 157: 254–260.
[18] Jia H L, Guo H, Guo M Z, Wang L C, Zhao J L, Fan X H. Finite element analysis of performance on elastic press wheel of row sowing plow machine for covering with soil and its experiment. Transactions of the CSAE, 2015; 31(21): 9–16. (in Chinese)
[19] Dai F, Song X F, Zhao W Y, Zhang F W, Ma H J, Ma M Y. Simulative calibration on contact parameters of discrete elements for covering soil on whole plastic film mulching on double ridges. Transactions of the CSAM, 2019; 50(2): 49–56, 77. (in Chinese)
[20] Ucgul M, Saundersa C, Li P L, Lee S H. Analyzing the mixing performance of a rotary spader using digital image processing and discrete element modelling (DEM). Computers and Electronics in Agriculture, 2018; 151: 1–10.
[21] Barr J B, Ucgul M, Desbiolles J M A, Fielke J M. Simulating the effect of rake angle on narrow opener performance with the discrete element method. Biosystems Engineering, 2018; 171: 1–15.
[22] Wang X Z, Zhang S, Pan H B, Zheng Z Q, Huang Y X, Zhu R X. Effect of soil particle size on soil-subsoiler interactions using the discrete element method simulations. Biosystems Engineering, 2019; 182: 138–150.
[23] Zhang S L, Zhao W Y, Dai F, Song X F, Qu J F, Zhang F W. Simulation analysis and test on suppression operation process of ridging and film covering machine with full-film double-furrow. Transactions of the CSAE, 2020; 36(1): 20–30. (in Chinese)